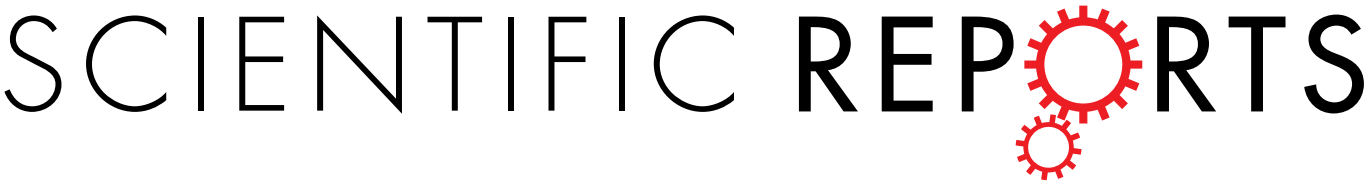

OPEN

Substructure-activity relationship studies on antibody recognition for phenylurea compounds using competitive immunoassay and computational chemistry

Received: 27 November 2017
Accepted: 29 January 2018
Published online: 15 February 2018

Fuyuan Zhang[1,3], Bing Liu[1], Guozhen Liu[3], Yan Zhang[1], Junping Wang[1] & Shuo Wang[1,2]

Based on the structural features of fluometuron, an immunizing hapten was synthesized and conjugated to bovine serum albumin as an immunogen to prepare a polyclonal antibody. However, the resultant antibody indicated cross-reactivity with 6 structurally similar phenylurea herbicides, with binding activities (expressed by IC_{50} values) ranging from 1.67 μg/L to 42.71 μg/L. All 6 phenylurea herbicides contain a common moiety and three different substitutes. To understand how these three different chemical groups affect the antibody-phenylurea recognition activity, quantum chemistry, using density function theory (DFT) at the B3LYP/6-311++ G(d,p) level of theory, was employed to optimize all phenylurea structures, followed by determination of the 3D conformations of these molecules, pharmacophore analysis, and molecular electrostatic potential (ESP) analysis. The molecular modeling results confirmed that the geometry configuration, pharmacophore features and electron distribution in the substituents were related to the antibody binding activity. Spearman correlation analysis further elucidated that the geometrical and electrostatic properties on the van der Waals (vdW) surface of the substituents played a critical role in the antibody-phenylurea recognition process.

Phenylurea herbicides constitute an important group of herbicides extensively utilized for herbaceous and perennial weed control in non-crop areas and for the preemergent treatment of fruit crops[1]. Globally, phenylurea herbicides have been detected in surface water[2], groundwater[3], soil and sediment[4] in areas where their extensive use occurred. Phenylurea herbicides are relatively long-lived in the environment, and their introduction to the food chain[5] via the environment is deemed a serious risk to human health[6]. Therefore, it is evident that environmental risk and food safety problems need to be mitigated.

Currently, immunoassays, such as enzyme-linked immunosorbent assay (ELISA), have been widely used in practice for the fast monitoring of pesticide residues in environmental or food samples[7,8]. However, individual small molecules always belong to one class of compounds, for instance, the phenylurea herbicide family[9], and most of the resultant antibodies elicited by one specific hapten carrier usually cross-react with other structural analogues[10,11]. This is particularly true if they share an identical or very similar epitope with the hapten used. The mechanism of the cross-reaction between antibodies and different analogues is difficult to elucidate. Although many studies have suggested an antibody recognition mechanism based on X-ray graphs of the antibody with a hapten, crystallization of the title antibody-hapten complex (particularly in polyclonal antibodies) has become a new challenge due to stringent experimental conditions[12–14].

Since the 1990s, computational chemistry, such as quantum chemistry and molecular mechanics methods, has been used for preliminary guidance on immunoassay development[15–17]. Computational chemistry not only provided a powerful method to explain the cross-reactivity but also became a useful tool to understand the

[1]Key Laboratory of Food Nutrition and Safety, Ministry of Education of China, Tianjin University of Science and Technology, Tianjin, 300457, China. [2]Beijing Advanced Innovation Center for Food Nutrition and Human Health, Beijing Technology & Business University (BTBU), Beijing, 100048, China. [3]Department of Molecular Sciences, ARC Centre of Excellence in Nanoscale Biophotonics (CNBP), Macquarie University, North Ryde, 2109, Australia. Correspondence and requests for materials should be addressed to S.W. (email: s.wang@tust.edu.cn)

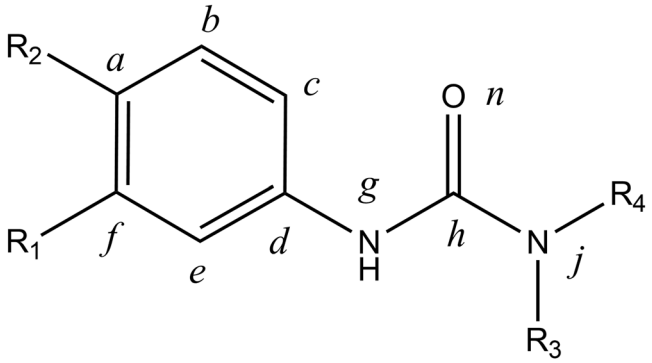

Figure 1. Common structure of the phenylurea molecules in this study. R_1, R_2 and R_3 represent different chemical groups in the different molecules, and R_4 represents the methyl group. *a-j* represent the number of atoms in the molecule.

Analytes	R_1	R_2	R_3	IC_{50} (μg/L)	CRs (%)
Fluometuron	$-CF_3$	-H	$-CH_3$	1.67	100.00
Neburon	-Cl	-Cl	$-CH_2CH_2CH_2CH_3$	2.41	69.40
Diuron	-Cl	-Cl	$-CH_3$	8.35	19.99
Chlorbromuron	-Cl	-Br	$-OCH_3$	9.77	17.10
Fenuron	-H	-H	$-CH_3$	11.61	14.38
Linuron	-Cl	-Cl	$-OCH_3$	42.71	3.91

Table 1. Structures, IC_{50} and CRs of the title phenylurea compounds. The antibody (with a better titer and cross-reactivity, 80000 U and 83.1%, respectively) obtained from number II rabbit was used to establish the ELISA method.

hapten-antibody recognition mechanism in the absence of antibody physicochemical information. In particular, 2D-QSAR or 3D-QSAR methods, such as CoMSIA and CoMFA Contour, have been used in many studies to investigate the binding activities of polyclonal[14,18,19] and monoclonal[20,21] antibodies against structurally similar compounds. These methods, however, are only suitable for broad-specific antibodies that can recognize a large number of targets and are not suitable for antibodies that only recognize several compounds[22].

In this study, a specific hapten was synthesized and conjugated to bovine serum albumin, as the immunogen, to produce a new anti-fluometuron polyclonal antibody. However, when we used the resultant antibody to develop a competitive ELISA, we encountered a general issue, as in most other immunoassays: the specific antibody could also recognize five other analogues with different activities. To explore how this antibody, elicited by one specific immunogen, could cross-react with other targets, the half maximal inhibitory concentration (IC_{50}) values, presented as the binding activity of the antibody, were calculated and analyzed. Subsequently, quantum chemistry and molecular mechanics methods were employed to explain how the substituents of the six phenylurea compounds caused the differences in binding activity. Lastly, the molecular surfaces were quantitatively analyzed to correlate the binding activities and the molecular surface descriptors of substituents in the phenylurea compounds.

Results

Antibody binding activity analysis. According to the two-dimensional structures of the phenylurea molecules (Fig. 1), the 6 title compounds were divided into three groups. The first group consisted of fluometuron and fenuron, which have different substitutes at the R_1 position. The second group contained neburon and diuron, which have different substitutes at the R_2 position. The third group included, chlorbromuron and linuron, which have different substitutes at the R_3 position.

We performed a direct competitive ELISA to evaluate the binding activity of the resultant antibody. IC_{50} and cross-reactivity (CRs) values were calculated to represent the binding activity and specificity of the antibody. These values are shown in Table 1.

The antibody with the best sensitivity to fluometuron ($IC_{50} = 1.67$ μg/L) was used as the hapten. Although the structure of fenuron and fluometuron are identical except for the substituted group at R_1, the IC_{50} value of fenuron (11.61 μg/L) is obviously different from that of fluometuron, and the specificity dropped dramatically from 100% (for fluometuron) to 11.61% (for fenuron). This indicates that the lack of $-CF_3$ group at the R_1 position limited the antibody recognition of fenuron. In the second group, neburon and diuron have very different structures from fluometuron, but the antibody has the ability to sensitively recognize them with IC_{50} values of 2.41 μg/L and 8.35 μg/L, respectively. The butyl group at the R_2 position in neburon is replaced by a methyl group in diuron, and this difference led to a more than 7-fold decrease in the binding activity. In the third group, the replacement of the chlorine atom by a bromine atom at the R_2 position in chlorbromuron ($IC_{50} = 9.77$ μg/L)

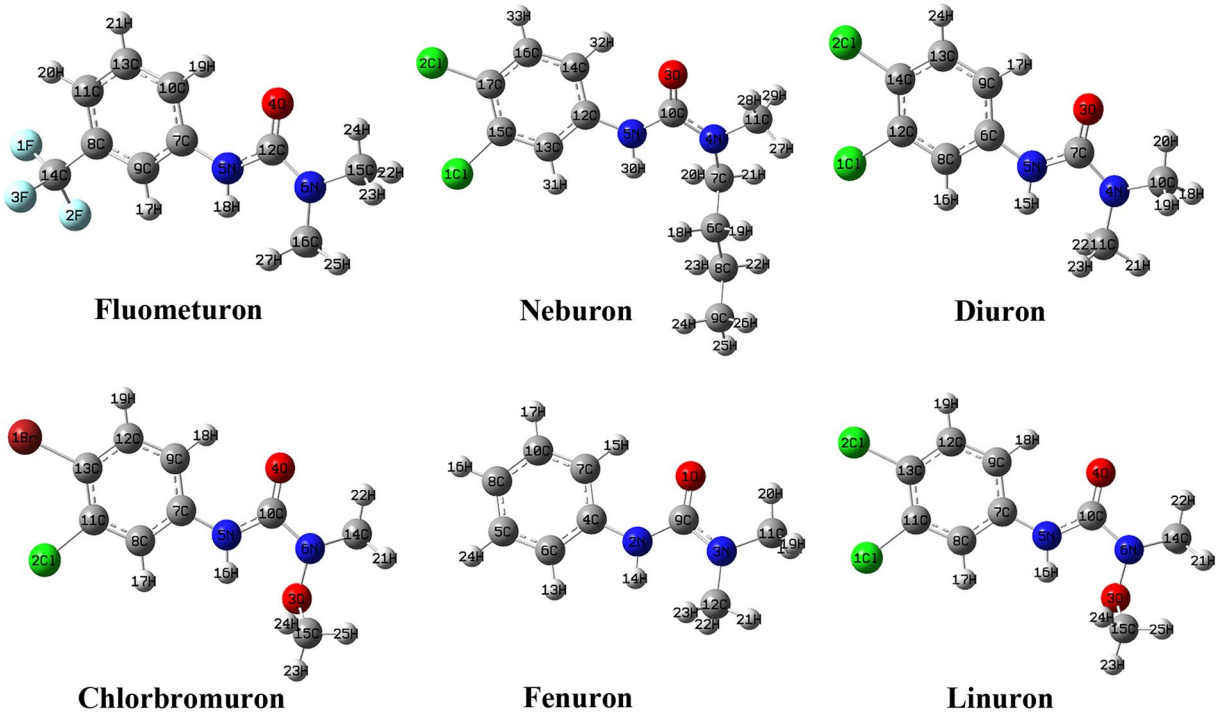

Figure 2. The optimized structures of phenylurea molecules at the DFT/B3LYP/6-311++ G(d,p) level of theory.

increased the antibody-chlorbromuron binding activity dramatically. In addition, the comparison of the binding activity to linuron ($IC_{50} = 42.71\,\mu g/L$) and diuron ($IC_{50} = 8.35\,\mu g/L$) suggested that the different groups at the R_3 position, where a methoxy group replaced the methyl group, could cause an obvious decline in antibody activity for linuron.

The ELISA results demonstrated that the differences in the hapten-antibody binding activity may be caused by the different substitutes in the otherwise structurally similar analytes. However, we cannot explain how different substitutes affect the binding ability just by examining the two-dimensional structural formulas. In the hapten-antibody recognition process, the 3D configuration of the hapten molecule should match that of the active pocket of the antibody, according to the geometric configuration matching mechanism[13,17,23]. Cross-reactions will occur if molecules have the same or similar geometric configuration as the hapten. To understand the recognition mechanism, the 3D configuration of phenylurea molecules were optimized (Fig. 2) and studied by employing quantum chemistry and molecular mechanics methods.

Conformational analysis and phenylurea molecules alignment. As seen from the optimized structures in Fig. 2, all molecules have similar bond lengths, bond angles and dihedral angles from atom *a* to atom *j*. Thus, they are well superposed based on their common structures, and the difference in the geometric configuration is mainly located in the different substitutes. Moreover, we can see that molecules in each group have a high degree of alignment based on their common structures (Fig. 3). In the first group, the fluometuron molecule has a very high fitting degree with fenuron based on their common structure (atoms *a*-*j*, R_2 and R_3), showing an alignment RMS value of 0.0190. Even so, the $-CF_3$ group at the R_1 position in fluometuron caused the carbon atoms on the phenyl ring to slightly bend out of the phenyl ring plane. This change contributes to an almost 7-fold gap in the IC_{50} value determined from the geometric configuration. We speculate that the antibody raised by fluometuron contained a $-CF_3$ complementary cavity, and this cavity could spatially recognize certain bulky groups, such as $-CF_3$.

For neburon, the existence of the bulky butyl group at the R_3 position also dramatically changed the general conformational structure that was exposed to the antibody, especially the dihedral angle of C_{10}-C_5-C_{12}-C_{13} (−164.4°). This value is obviously smaller than those of the other 5 molecules (are all more than 174.0°), and the steric hindrance of the butyl group caused the whole neburon molecule be poorly aligned with the diuron molecule (the alignment RMS value was only 0.9346). Furthermore, neburon shows a better binding ability than diuron. For the third group, the alkoxy group at the R_3 position in the chlorbromuron and linuron molecules also affects the spatial conformation of the methyl group at the R_4 position. Chlorbromuron has a high degree of alignment with linuron, and the alignment RMS value is 0.0106. However, the replacement of the chlorine atom by a bromine atom at the R_2 position resulted in the bond angles of C_1-C_{13}-C_{11} (122.2°) and C_2-C_{11}-C_{13} (121.9°) in chlorbromuron being larger than those in linuron. This scenario contributes to an almost 4-fold activity gap in the binding activity. The geometric configuration analysis shows that certain bulky chemical group at the R_1 and R_3 positions play a positive role the antibody-phenylurea binding process. Moreover, the antibody binding sites can also accurately recognize variations of the common structures of these molecules, resulting in differences in binding activity.

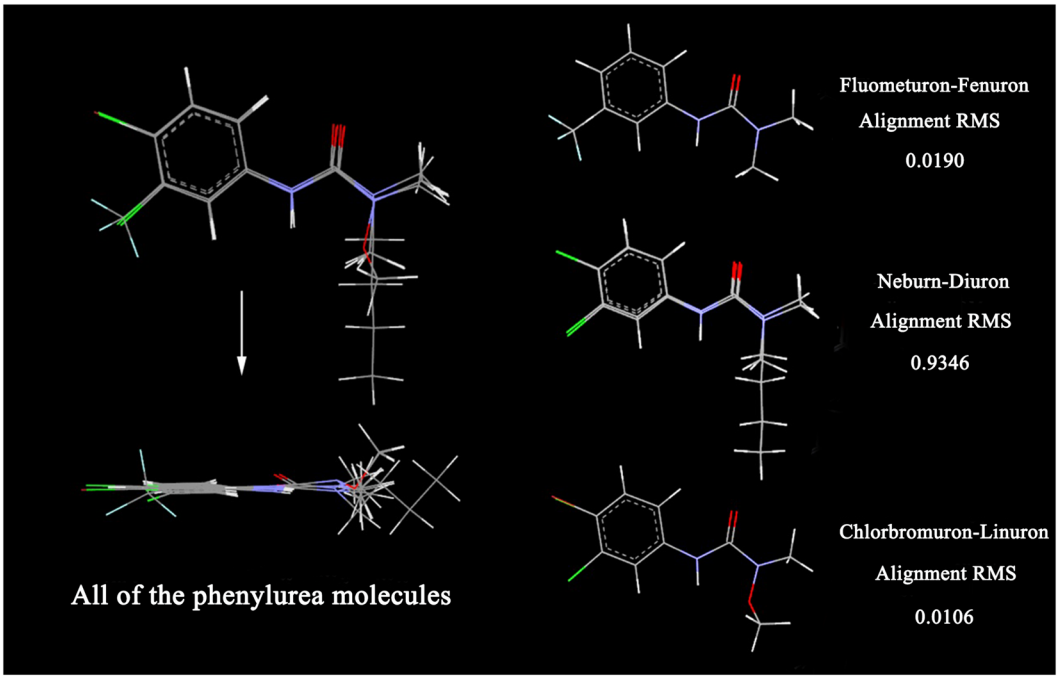

Figure 3. The superposition graph of the phenylurea molecules. Gray sections represent carbon atoms, white represent hydrogen atoms, light blue represent fluorine atoms, blue represent nitrogen atoms, green represent chlorine atoms, red represent oxygen atoms and brown represent bromine atoms.

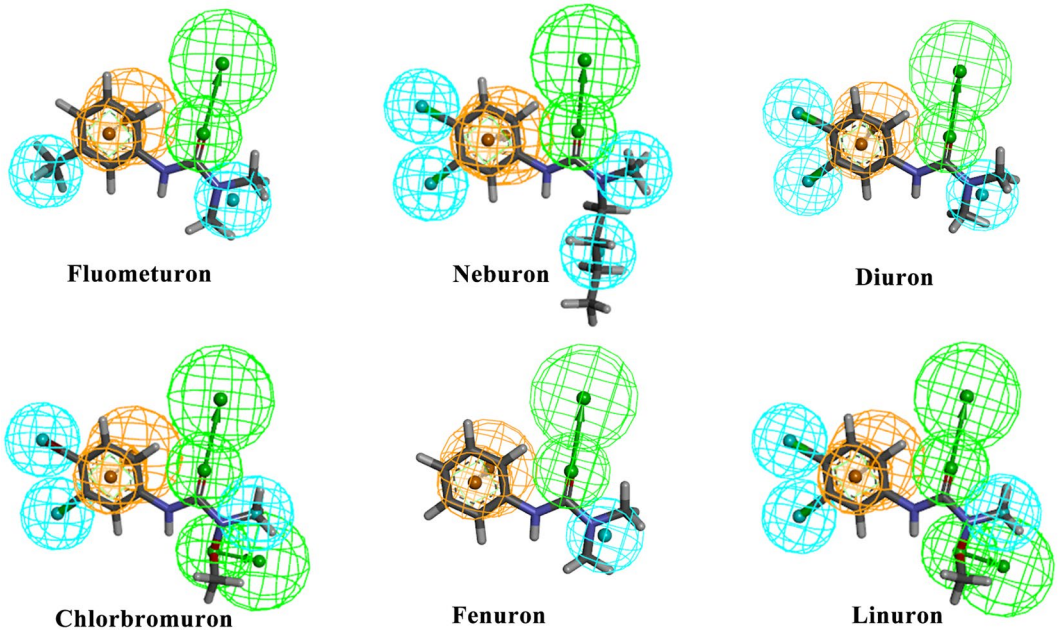

Figure 4. The pharmacophore chemical features mapped onto the phenylurea molecules. The chemical features are color coded, with light blue representing hydrophobic features, orange representing ring aromatic features and green representing hydrogen-bond acceptors.

Pharmacophore model analysis. Fig. 4 shows the pharmacophore models of the phenylurea molecules. The pharmacophore is an ensemble of steric and electronic features of the molecule, such as hydrophobic centroids, hydrogen-bond acceptors or donors and aromatic rings, which are necessary for molecular recognition of a ligand by a biological macromolecule[24,25]. The pharmacophore model of each phenylurea molecule had an aromatic ring feature in the phenyl ring area, a hydrophobic centroid at the R_4 position and a hydrogen-bond acceptor at the carbonyl group position. The $-CF_3$ group at the R_1 position in fluometuron serves as a hydrophobic centroid. Simultaneously, the chemical features of neburon indicate that it cannot align well with diuron, though

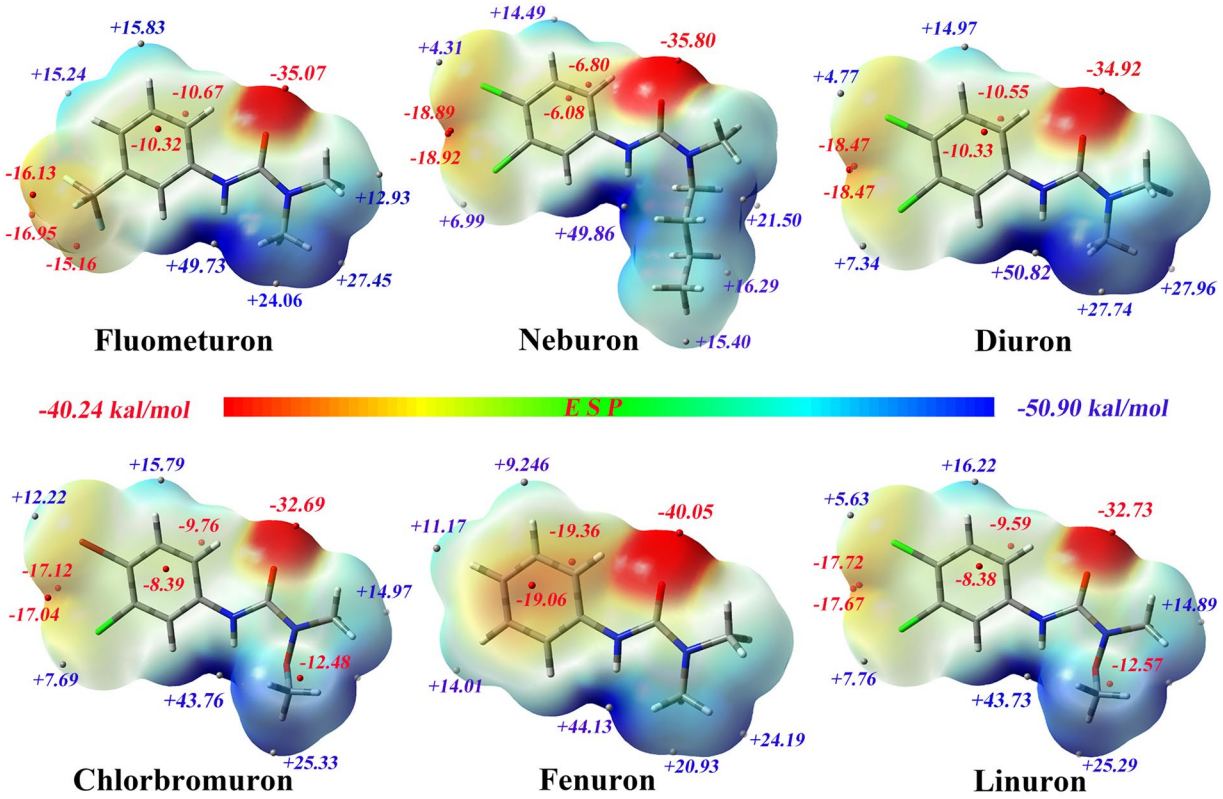

Figure 5. The structures optimized by DFT and the ESP of the phenylurea molecules on the 0.001 a.u. contours of the electronic density of the molecules. The negative ESP regions are indicated in red, and the positive regions in blue. Potential is coded in the following order: red < orange < yellow < green < blue. The red and white spheres represent the minima and maxima of the ESP on the vdW surface.

their only difference is located at the R_3 group; the hydrophobicity of the butyl group may influence the steric configuration of the whole neburon molecule, resulting in a higher activity ($IC_{50} = 2.41\,\mu g/L$) than that of diuron. The chlorbromuron molecule has the same pharmacophore features as linuron but with a bromine atom, and all chlorine atoms serve as hydrophobic centroids. However, we cannot offer a reason for the different activities based simply on pharmacophore features. Except for the R_3 group, linuron has the same structure as neburon, but the oxygen atom in the R_3 group in the linuron molecule serves as a hydrogen-bond donor. This led to a decrease in activity, as suggested by the pharmacophore features.

There are some limits in exploring the activity differences according to the pharmacophore analysis. For example, the bromine atom in chlorbromuron and the chlorine atom in linuron serve as hydrophobic centroids, yet we cannot distinguish the differences between them. Furthermore, the hydrogen-bonding and hydrophobic interactions were essentially caused by the electron distribution on the molecular surface[26]. In this way, ESP is also an important and indispensable parameter in the study of the hapten-antibody recognition mechanism.

Molecular electrostatic potential analysis. The ESP has a unique role in the prediction and analysis of molecular recognition and is often helpful in demonstrating non-covalent molecular interaction properties[27,28]. By employing the ESP surface, we can determine the spatial regions in the molecular structure at which the molecular electrostatic potential is negative or positive. This helps visualize charged regions of a molecule and is qualitatively useful in the analysis of electrostatic interactions between the antibody and the title compound[13,29].

Three-dimensional plots of the molecular electrostatic potentials of the phenylurea compounds are illustrated in Fig. 5. The ESP surface depicts the phenylurea compound size, configuration, and charge density. The ESP color code ranges from −40.24 to +50.90 kcal/mol. In addition, the minima and maxima of the ESP on the vdW surface were analyzed by Multiwfn and mapped onto the surface of the molecules. All the phenylurea compounds have areas of positive potential at the front of the hydrogen atoms arising from the lower electronegativity of these atoms. This is comparable to carbon or nitrogen atoms, and the most positive potential area (show in dark blue) is located on the surface of the hydrogen atoms associated with nitrogen atoms, where the global maximum point is located. These positive regions can be easily attracted by the negative potential regions of the antibody binding sites. The most negative ESP region (shown in dark red), with a global minimum lower than −32.6 kcal/mol, is located at the front of the carbonyl oxygen atoms. This large negative value is due to the lone pair of electrons on oxygen, which means that this region can be easily attracted by the region of positive potential. The ESP over the phenyl ring carbons is moderately negative, and two minima with similar values are located above and below the ring, reflecting the abundant π electrons of the phenyl ring. As the R_1 and R_2 substituents are all

Group	Method	*S*	S^+	S^-	*P*	*I*	*A*	*Va*	Va^+	Va^-	*B*
R_1	Spearman Correlation	−0.667	0.943**	−0.943**	0.943**	0.314	0.943**	0.314	0.943**	−0.2	0.841*
	Sig. (2-tailed)	0.148	0.005	0.005	0.005	0.544	0.005	0.544	0.005	0.704	0.036
R_2	Spearman Correlation	0.143	−0.029	0.086	0.314	0.174	−0.029	−0.143	−0.086	0.086	0.600
	Sig. (2-tailed)	0.787	0.9572	0.872	0.544	0.742	0.957	0.787	0.872	0.872	0.208
R_3	Spearman Correlation	0.257	−0.086	0.671	0.872	0.714	−0.257	0.754	0.257	0.872	0.621
	Sig. (2-tailed)	0.623	0.872	0.215	0.0539	0.111	0.623	0.084	0.623	0.054	0.188

Table 2. Spearman correlation analysis for molecule fragments ESP descriptors and antibody binding ability (expressed by IC_{50} values). **Correlation is significant at 0.01 level (2-tailed). *Correlation is significant at 0.05 level (2-tailed).

electron-withdrawing groups, under the influence of the electron-attracting effect created by groups R_1 and R_2, the electron distribution over the phenyl ring also changed.

There are no electron-withdrawing groups associated with the phenyl ring in fenuron, so more electrons are around its phenyl ring than around those of the other five phenylurea molecules. In addition, the minimum values in this area are −19.06 and −19.36 kcal/mol. For fluometuron, the -CF_3 group, an electron-withdrawing group, attract some electrons around the phenyl ring, resulting in a moderate electron density and three minimum points in front of the R_1 group, and this -CF_3 group also led a decrease in the electron density and minimum ESP value around the phenyl ring. We further speculated that the electron-withdrawing group at the R_1 position could change the electron distribution around the phenyl ring and the R_1 region, and this was reflected in the higher selectivity for the antibody by electrostatic interaction.

Molecules in the second group have almost identical surface charges, except for in the region of the R_3 group. As the electron-withdrawing effect is caused by chlorine atoms, there is a high electron density area and two ESP minima between the R_1 and R_2 groups. However, the four-carbon chain in neburon changes the electron distribution around the R_3 position, resulting in a lower electron density and several lower ESP maxima (+15.40 to +21.50 kcal/mol) compared with diuron (electron density of +22.95 and the ESP maxima of +27.74 kcal/mol and +27.96 kcal/mol). This indicates that the alkyl chain could scatter the electron distribution of the R_3 position and increase the antibody-phenylurea binding activity.

The alkoxy group in linuron reduced the binding activity, possibly because the oxygen atom attracted electrons around it and shared the electrons around the carbonyl group, resulting in a moderate electron density and a minima (−12.57 kcal/mol) around the alkoxy group. Compared with linuron, chlorbromuron also has an alkoxy group at the R_3 position. However, the chlorine atom at the R_2 position in linuron has a stronger electron-withdrawing ability than the bromine atom at R_2 in chlorbromuron. Thus, chlorbromuron has a lower electron density and smaller minima in this area, and the change in the charge distribution may result in the difference in activity.

Quantitative analysis of the molecular surface. Weak interactions in biochemical systems can be well predicted and explained by analyzing the ESP descriptors on the molecular surface[30,31]. The quantitative analysis of the molecular surfaces in this study is summarized in Table S1. The Spearman correlation analysis between the molecular fragment descriptors and antibody activity (IC_{50} values) is summarized in Table 2. We can see that the parameters – including S^+, *P*, *A*, Va^+ and *B* of the R_1 group; *B* of the R_2 group; and S^-, *P*, *I*, *Va*, Va^- and *B* of the R_3 group – have a positive relationship with the antibody activity, while *S* and S^- of the R_1 group have a negative relationship with antibody activity. Among these parameters, *B* of the R_1 group has a key relationship with the antibody activity coefficient, which is significant at the 0.01 level (2-tailed). S^+, S^-, *P*, *A* and Va^+ of the R_1 group also have a crucial relationship with the antibody activity coefficient. All are significant at the 0.05 level. The results showed that the antibody binding activity is linked to geometrical and electrostatic descriptors on the surfaces of the phenylurea molecules, particularly the substituent groups. Specifically, the R_1 and R_3 groups played a key role in the antibody-phenylurea binding process.

Discussion

In summary, ELISA analysis confirmed that the obtained antibody could recognize six structurally similar analogs. By analyzing the geometrical conformation and physicochemical properties of the optimized structures, we speculated that the antibody binding pocket could recognize slight differences in the geometric conformation of the molecules. In addition, the negative electrostatic potential of the hydrophobic -CF_3 group at the R_1 position and the hydrophobic butyl group at the R_3 position also contributed to the molecule-antibody binding activity. Meanwhile, the alkoxy group, which served as hydrogen-bond donor, at the R_3 position decreased the binding activity. Through Spearman correlation analysis between the molecular descriptors and antibody activity, we found that S^+, S^-, *P*, *A*, Va^+ and *B* of the R_1 group had key relationships with the antibody activity. The results indicated that the geometrical and electrostatic properties on the vdW surface of the R groups, especially the R_1 and R_3 groups, played a key role in the antibody-phenylurea binding activity. This investigation demonstrated that we could explore the antibody recognition mechanism using computational chemistry techniques, despite lacking structural information of the antibody. This study also draws attention to the need to design new haptens to produce specific or broad-spectrum antibodies in the future.

Methods

Antibody preparation. In this study, a hapten with a three-carbon spacer arm was synthesized, and then, an immunogen- and enzyme-labeled antigen was obtained by conjugating the hapten to BSA and HRP via the active ester method. The hapten-BSA conjugates were used as the immunogen to immunize two 3-month-old male New Zealand white rabbits (numbers I and II). After the initial immunization and four additional immunizations, the rabbits were sacrificed, and the sera were obtained by centrifugation. Aliquots of the sera were stored at 4 °C in 50% saturated ammonium sulfate. Subsequently, the antibodies were purified by Protein A-Sepharose 4B immunoaffinity chromatography.

Direct competitive ELISA protocol. The resulting antibodies were evaluated by a conventional direct competitive ELISA method. First, 0.25 μg/well of antibody was coated on a polystyrene 96-well plate using 100 μL/well of coating buffer (0.05 mol/L $NaHCO_3$, pH 9.6). After overnight incubation at 4 °C, the excess binding sites were blocked by 200 μL of a blocking solution at 37 °C for 1 h. Then, a mixture of the standard solution and hapten-HRP solution were simultaneously added to each well. After 1 h of competing reaction at 37 °C, substrates A and B were added sequentially for coloration. Finally, the enzymatic reaction was stopped by adding 2 mol/L H_2SO_4. The absorbance was determined at a primary wavelength of 450 nm, with a reference wavelength of 650 nm, using a microplate reader. After each step, 250 μL of PBST (10 mM PBS, pH 7.4, 0.05% Tween-20) was used to wash the plate. IC_{50} and cross-reactivity (CR) values were calculated to evaluate the activity of the resulting antibody[13,18,32].

Calculation of the antibody binding activity. Inhibition ratios and IC_{50} values were calculated. The inhibition ratio was defined by the following equation:

$$Inhibition\ ratio = \frac{A_{Inhibit} - A_{Blank}}{A_{Control} - A_{Blank}} \times 100\%$$

For this equation, $A_{Control}$ represents the absorbance value of the control group and $A_{Inhibit}$ and A_{Blank} represent the absorbance values of the inhibited group and blank group, respectively. The IC_{50} (μg/L) value was the analyte concentration when the inhibition ratio was 50%.

Geometry optimization and moleculars alignment. All structures were built in Gaussian 09 ES64L-G09RevE.01 (Gaussian, Wallingford, CT, USA) according to the phenylurea configurations in the Pubchem database. Then, DFT calculations with the B3LYP functional and 6-311++ G(d,p) basis set were performed to optimize the molecules using the Gaussian 09 package[13,33]. There were no imaginary frequencies for all structures, ensuring the local minimum was found. The Molecule Overlay dialog in Discovery Studio 2016 (Accelrys Software, Inc., San Diego, CA, USA) was used to conduct the three-dimensional molecular alignment. The alignment root-mean-square (RMS) value was introduced to measure the degree of molecular superposition in each group.

Pharmacophore model analysis. The Auto Pharmacophore Generation protocol in Discovery Studio 2016 was employed in this study. This protocol generated ten pharmacophore models for each molecule, and we chose the best one for analysis.

Molecular electrostatic potential analysis. The Gaussian 09 and Gaussian View 5 packages were employed to conduct the molecular electrostatic potential (ESP) analysis of the title compounds. Minima and maxima of the ESP were generated in the Multiwfn software package and mapped onto the vdW surface.

Quantitative analysis of the molecular surface. By defining the specific chemical groups (R_1, R_2 and R_3) in the Multiwfn package, descriptors were calculated. Spearman correlation via SPSS software served to detect relationships between molecular descriptors of the molecular fragments of phenylurea and the recognition ability (IC_{50}) of a polyclonal antibody.

References

1. Wang, D. *et al*. Phenylurea herbicide sorption to biochars and agricultural soil. *J Environ Sci Health B* **50**, 544–551 (2015).
2. Barchanska, H. *et al*. Atrazine, triketone herbicides, and their degradation products in sediment, soil and surface water samples in Poland. *Environ Sci Pollut Res Int* **24**, 644–658 (2017).
3. Fingler, S. *et al*. Herbicide micropollutants in surface, ground and drinking waters within and near the area of Zagreb, Croatia. *Environ Sci Pollut Res Int* **24**, 11017–11030 (2017).
4. Guo, J. *et al*. Occurrence of Atrazine and Related Compounds in Sediments of Upper Great Lakes. *Environ Sci Technol* **50**, 7335–7343 (2016).
5. Wu, J. *et al*. Triphenylamine-based hypercrosslinked organic polymer as adsorbent for the extraction of phenylurea herbicides. *J Chromatogr A* **1520**, 48–57 (2017).
6. Dong, X., Liang, S., Shi, Z. & Sun, H. Development of multi-residue analysis of herbicides in cereal grain by ultra-performance liquid chromatography-electrospray ionization-mass spectrometry. *Food Chem* **192**, 432–440 (2016).
7. Sharma, P., Sablok, K., Bhalla, V. & Suri, C. R. A novel disposable electrochemical immunosensor for phenyl urea herbicide diuron. *Biosens Bioelectron* **26**, 4209–4212 (2011).
8. Bhalla, V., Sharma, P., Pandey, S. K. & Suri, C. R. Impedimetric label-free immunodetection of phenylurea class of herbicides. *Sensors and Actuators B: Chemical* **171–172**, 1231–1237 (2012).
9. Yuan, M. *et al*. Immunoassay for phenylurea herbicides: application of molecular modeling and quantitative structure-activity relationship analysis on an antigen-antibody interaction study. *Anal Chem* **83**, 4767–4774 (2011).
10. Cui, Y. *et al*. Hapten synthesis and monoclonal antibody-based immunoassay development for the analysis of thidiazuron. *Journal of Plant Growth Regulation* **35**, 357–365 (2015).

11. Zhao, F. *et al*. Development of a biotinylated broad-specificity single-chain variable fragment antibody and a sensitive immunoassay for detection of organophosphorus pesticides. *Anal Bioanal Chem* **408**, 6423–6430 (2016).
12. He, K. *et al*. Crystal Structure of the Fab Fragment of an Anti-ofloxacin Antibody and Exploration of Its Specific Binding. *J Agric Food Chem* **64**, 2627–2634 (2016).
13. Wang, Z., Luo, P., Cheng, L., Zhang, S. & Shen, J. Hapten-antibody recognition studies in competitive immunoassay of alpha-zearalanol analogs by computational chemistry and Pearson Correlation analysis. *J Mol Recognit* **24**, 815–823 (2011).
14. Mu, H. *et al*. Stereospecific recognition and quantitative structure-activity relationship between antibodies and enantiomers: ofloxacin as a model hapten. *Analyst* **140**, 1037–1045 (2015).
15. Xu, Z. L. *et al*. Application of computer-assisted molecular modeling for immunoassay of low molecular weight food contaminants: A review. *Anal Chim Acta* **647**, 125–136 (2009).
16. Pantazes, R. J. & Maranas, C. D. OptCDR: a general computational method for the design of antibody complementarity determining regions for targeted epitope binding. *Protein Eng Des Sel* **23**, 849–858 (2010).
17. Li, X. *et al*. Molecular characterization of monoclonal antibodies against aflatoxins: a possible explanation for the highest sensitivity. *Anal Chem* **84**, 5229–5235 (2012).
18. Zeng, H. *et al*. Broad-Specificity Chemiluminescence Enzyme Immunoassay for (Fluoro)quinolones: Hapten Design and Molecular Modeling Study of Antibody Recognition. *Anal Chem* **88**, 3909–3916 (2016).
19. Chen, J. *et al*. Investigation of an Immunoassay with Broad Specificity to Quinolone Drugs by Genetic Algorithm with Linear Assignment of Hypermolecular Alignment of Data Sets and Advanced Quantitative Structure-Activity Relationship Analysis. *J Agric Food Chem* **64**, 2772–2779 (2016).
20. Wang, Z., Kai, Z., Beier, R. C., Shen, J. & Yang, X. Investigation of antigen-antibody interactions of sulfonamides with a monoclonal antibody in a fluorescence polarization immunoassay using 3D-QSAR models. *Int J Mol Sci* **13**, 6334–6351 (2012).
21. Mu, H. *et al*. Molecular modeling application on hapten epitope prediction: an enantioselective immunoassay for ofloxacin optical isomers. *J Agric Food Chem* **62**, 7804–7812 (2014).
22. Zhang, Y. F., Ma, Y., Gao, Z. X. & Dai, S. G. Predicting the cross-reactivities of polycyclic aromatic hydrocarbons in ELISA by regression analysis and CoMFA methods. *Anal Bioanal Chem* **397**, 2551–2557 (2010).
23. Dengl, S. *et al*. Hapten-directed spontaneous disulfide shuffling: a universal technology for site-directed covalent coupling of payloads to antibodies. *FASEB J* **29**, 1763–1779 (2015).
24. Aparoy, P., Kumar Reddy, K., Kalangi, S. K., Chandramohan Reddy, T. & Reddanna, P. Pharmacophore modeling and virtual screening for designing potential 5-lipoxygenase inhibitors. *Bioorg Med Chem Lett* **20**, 1013–1018 (2010).
25. Brahmachari, G., Choo, C., Ambure, P. & Roy, K. *In vitro* evaluation and *in silico* screening of synthetic acetylcholinesterase inhibitors bearing functionalized piperidine pharmacophores. *Bioorg Med Chem* **23**, 4567–4575 (2015).
26. Contreras-Garcia, J., Yang, W. & Johnson, E. R. Analysis of hydrogen-bond interaction potentials from the electron density: integration of noncovalent interaction regions. *J Phys Chem A* **115**, 12983–12990 (2011).
27. Chiu, T. P., Rao, S., Mann, R. S., Honig, B. & Rohs, R. Genome-wide prediction of minor-groove electrostatic potential enables biophysical modeling of protein-DNA binding. *Nucleic Acids Res* (2017).
28. McCaughan, J. A., Turner, D. M. & Battle, R. K. Electrostatic Potential Change in a Paired Epitope: A Novel Explanation for Bw4 Antibodies in Patients With B13 (Bw4) Antigens. *Transplantation* **100**, e32–34 (2016).
29. Zhanhui, W. *et al*. Development of a monoclonal antibody-based broad-specificity ELISA for fluoroquinolone antibiotics infoods and molecular modeling studies of cross-reactive compounds. *Anal Chem* **79**, 4471–4483 (2007).
30. Lu, T. & Chen, F. Quantitative analysis of molecular surface based on improved Marching Tetrahedra algorithm. *J Mol Graph Model* **38**, 314–323 (2012).
31. Tian, L. & Sergio, M. Wavefunction and reactivity study of benzo[a]pyrene diol epoxide and its enantiomeric forms. *Struct Chem* **25**, 1521–1533 (2014).
32. Garcia-Fernandez, J., Trapiella-Alfonso, L., Costa-Fernandez, J. M., Pereiro, R. & Sanz-Medel, A. A quantum dot-based immunoassay for screening of tetracyclines in bovine muscle. *J Agric Food Chem* **62**, 1733–1740 (2014).
33. Arshad, M. N. *et al*. Synthesis, crystal structure, spectroscopic and density functional theory (DFT) study of N-[3-anthracen-9-yl-1-(4-bromo-phenyl)-allylidene]-N-benzenesulfonohydrazine. *Spectrochim Acta A Mol Biomol Spectrosc* **142**, 364–374 (2015).

Acknowledgements

The authors are grateful for the financial support from the National Natural Science Foundation of China (31301462). We also greatly appreciate the financial support from Tianjin Municipal Science and Technology Commission (Project No. 16PTSYJC00130) and International Science and Technology Cooperation Program of China (Project No. 2014DFR30350).

Author Contributions

F.Z. conducted the experiments, results analysis and manuscript writing; B.L. and G.L. conducted the instruction of experiments; Y.Z., J.W. and S.W. reviewed the manuscript.

Additional Information

Supplementary information accompanies this paper at https://doi.org/10.1038/s41598-018-21394-x.

Competing Interests: The authors declare no competing interests.

Publisher's note: Springer Nature remains neutral with regard to jurisdictional claims in published maps and institutional affiliations.